CONTENTS

NASA Technical Paper 1288

Microstructure and Mechanical Properties of Quenched and Tempered 300M Steel

J. L. Youngblood and M. Raghavan

AUGUST 1978

NASA

NASA Technical Paper 1288

Microstructure and Mechanical Properties of Quenched and Tempered 300M Steel

J. L. Youngblood
Lyndon B. Johnson Space Center
Houston, Texas

M. Raghavan
Olin Corporation
New Haven, Connecticut

NASA
National Aeronautics
and Space Administration

Scientific and Technical
Information Office

1978

Blank Page

TABLES

FIGURES

SUMMARY

Type 300M steel was subjected to a wide range of quenched and tempered heat treatments. The plane-strain fracture toughness and the tensile ultimate and yield strengths were evaluated. Cryogenic mechanical properties were obtained for conventionally heat-treated steel. The microstructure of all heat-treated test coupons was studied both optically and by transmission electron microscopy. Fracture surfaces were studied by means of scanning electron microscopy.

Results indicate that substantial improvement in toughness with no loss in strength can be accomplished in quenched and tempered steel by austenitizing at 1255 K (1800° F) or higher. Low fracture toughness in conventionally austenitized 300M steel (1144 K (1600° F)) appears to be caused by undissolved precipitates, seen both in the submicrostructure and on the fracture surface, which promote failure by quasi-cleavage. These precipitates appeared to dissolve in the range 1200 to 1255 K (1700° to 1800° F).

INTRODUCTION

The correlation of microstructure with mechanical properties of structural materials has been a topic of interest for many years, attracting the attention of numerous workers (refs. 1 to 20). Most of these studies have been focused primarily on either mechanical properties or microstructural details, and as a result, many ambiguities and unresolved questions remain. It is believed to be of utmost importance that equal emphasis be placed on both microstructure and mechanical behavior; the present investigation was undertaken with this dual emphasis as its cornerstone.

Type 300M steel has been selected for the landing gear on the NASA Space Shuttle Orbiter as well as on many conventional aircraft. Hence, optimizing its heat treatment to obtain the best combination of strength and toughness is of practical importance. Considerable research has already been conducted on 300M steel (refs. 10 and 21 to 24), but these studies have not dealt with the entire spectrum of available heat treatments. The present research is an attempt to add to these earlier studies by exploring in depth the influence of conventional quenching and tempering treatments[1] over as wide a temperature range as is practical for steels. In addition, to clarify the relative contributions of grain size and undissolved particles to fracture toughness, a dual-austenitizing treatment designed to produce both large grains and undissolved particles was investigated. To approximate industrial applications, relatively large section thicknesses were used throughout the study. The influence of each heat treatment was evaluated in terms of (1) the tensile

strength and fracture toughness and (2) the microstructure and fracture surface morphology. Limited testing was performed at cryogenic temperatures.

On the basis of the results thus obtained, explanations are offered as to the mechanisms responsible for the observed mechanical behavior. Heat treatments that should give an optimum combination of strength and toughness in practical applications are also recommended.

The heat treatments were performed by Advanced Technology Center, Inc., Dallas, Texas, under the direction of Dr. Roger D. Goolsby. Dr. Raghavan's contributions to this research were made possible through an NASA-sponsored NAS/NRC Postdoctoral Resident Research Associateship.

As an aid to the reader, where necessary the original units of measure have been converted to the equivalent value in the Systeme International d'Unites (SI). The SI units are written first, and the original units are written parenthetically thereafter.

EXPERIMENTAL PROCEDURE

Materials and Heat Treatment

The 300M steel used in the present study was obtained from a vendor[2] and met the specifications of AMS-6416. It was vacuum arc melted with a chemical composition given by the manufacturer as 0.41 carbon, 1.65 silicon, 0.65 manganese, 0.002 sulfur, 0.008 phosphorus, 0.78 chromium, 1.10 vanadium, 1.77 nickel, and 0.42 molybdenum. Approximately 2.3×10^5 grams (500 pounds) of steel were obtained in two different forms: (1) 0.0762- by 0.0127-meter (3 by 0.5 inch) section bar stock and (2) 0.0762- by 0.0254-meter (3 by 1 inch) section bar stock. All material had been normalized at 1183 K (1670° F) for 1 hour before delivery.

---

[1]Conventional quenching and tempering refers to that treatment wherein a steel object is first heated to a temperature high enough to convert the structure to the face-centered-cubic or austenite phase. It is then quenched directly into an oil bath at approximately 323 K (120° F). Tempering is then performed by heating the steel to a temperature slightly above room temperature but below the austenite transformation temperature. Usually, the piece of steel is heated in this manner for 2 hours, quenched into oil, and then reheated and quenched a second time under the same conditions. For convenience, the tempering treatments are often given an abbreviated description such as "2 plus 2 at 600° F" (2 hours at 589 K (600° F) - quenched into oil - 2 hours at 589 K (600° F) - quenched into oil).

[2]Latrobe Steel Company, Latrobe, Pa. 15650.

For the single-austenitizing heat treatments, specimens were austenitized for 1 hour in a vertical tube furnace in a continuously flowing helium atmosphere. This furnace had a uniform heat zone of 0.3 meter (12 inches), which was verified by hardness readings taken over the entire length of a tensile sample. Heated samples were directly quenched in oil at room temperature and double tempered (2 plus 2 hours) in a salt bath (oil quenched after each tempering treatment). Temperatures used were as follows.

Austenitizing temperature, K (°F)	Tempering temperature for each austenitizing temperature, K (°F)
1144 (1600)	Untempered
1255 (1800)	477 (400)
1366 (2000)	589 (600)
1477 (2200)	700 (800)
	811 (1000)

The dual-austenitizing experiments involved heat treating specimens 1 hour at 1477 K (2200° F) in a vertical tube furnace, dropping them directly into a second tube furnace held at 1144 K (1600° F) for 1 hour, and finally oil quenching them to room temperature. Subsequently, these specimens were tempered the same way as the single-austenitized specimens.

Test Specimens and Test Procedures

Compact tension fracture toughness specimens conforming to standards of the American Society for Testing and Materials (ASTM) were used for fracture toughness evaluation. Specimens were machined from both sizes of bar stock in the long transverse orientation. The tension specimens were machined from the same material and had nominal square cross sections of either 0.0127 by 0.0127 meter (0.5 by 0.5 inch) or 0.0254 by 0.0254 meter (1 by 1 inch).

Fracture tests were performed using a crack-opening displacement gage following the procedure outlined in ASTM E399-72 (revised). A 0.0254-meter (1 inch) extensometer (10 percent strain calibrated) or a strain gage (or both) were mounted on the gage section of the tension specimens to record strain during the tests.

In the cryogenic tests, specimens were cooled in an insulated chamber by a continuous flow of liquid nitrogen through copper tubes in the chamber. Temperature stability was obtained by controlling the flow of liquid nitrogen with a control band of ±3 K (±5° F). The temperature was monitored by installing two thermocouples; one measured the ambient temperature in the chamber and the other (bonded onto the specimen) measured the specimen temperature.

Metallography and Electron Microscopy

Specimens for optical microscopy and transmission electron microscopy (TEM) were carefully cut from the grip section of the tested tensile specimens. Specimens for TEM were prepared by thinning specimens chemically to 1.27×10^{-4} meter (0.005 inch) and jet polishing them to perforation (ref. 25). These specimens were examined in a JEM 7 electron microscope using a 100-kilovolt electron gun potential. Fracture toughness failure surfaces were cleaned by repeated washings with acetone, dried, and examined directly in a Cambridge Sterescan S4 scanning electron microscope using a 30-kilovolt electron gun potential. High-resolution fracture surfaces were prepared by coating with approximately 30 nanometers (300 angstroms) of gold. These were observed using a 20-kilovolt potential.

RESULTS

Mechanical Properties

The discussion of mechanical properties results consists of quenching and tempering effects, dual-austenitizing treatments, and cryogenic tests.

Quenched and tempered steels.- Figures 1 to 3 are plots based on single-point data of the effect of tempering on the strength and toughness of the steel. The fracture toughness and the ultimate strength were observed to be independent of thickness so that figures 1 and 3 represent the response of both sample groups. It was impossible to combine all the yield strength results from the 0.0127-meter (0.5 inch) bar stock with those of the 0.0254-meter (1 inch) material. Actual data from which these curves were derived are presented in tables I and II. One can readily see from figure 1 that it is possible to separate the specimens into two groups based on the fracture toughness response of the steel to tempering temperature. For convenience, specimens quenched from 1144 K (1600° F) will be referred to as class A specimens and all those quenched from higher temperatures will be referred to as class B specimens.

The curves indicate the following conditions. Fracture toughness of the class A specimens increases monotonically with tempering temperature; this increase is very gradual below 700 K (800° F). In contrast, fracture toughness of the class B specimens increases rapidly with tempering temperatures to approximately 477 K (400° F) but then declines sharply, reaching a minimum in toughness at approximately 700 K (800° F), and finally increases again with higher tempering temperatures to 811 K (1000° F). No parallel differences between these two classes of specimens were observed in the tensile properties shown in figures 2 and 3. All specimens showed increasing yield strengths with tempering temperatures to 589 K (600° F), with mixed behavior at higher temperatures. The ultimate tensile strengths invariably decreased with higher tempering temperatures. The results are in partial agreement with earlier work (refs. 6 and 22) done on 300M steel.

It is important to note at this stage that most of the data published on toughness have been obtained using Charpy V-notch tests. Though there is no direct quantitative correlation between published Charpy values and the present plane-strain fracture toughness values, a reasonable qualitative comparison can be made in many cases. Bucher et al. (ref. 22) studied the impact energy of 300M steel austenitized 1 hour at 1177 K (1660° F), oil quenched, and tempered 2 hours at 505 K (450° F), 602 K (625° F), 661 K (730° F), 744 K (880° F), and 866 K (1100° F). Their curve of impact energy as a function of tempering temperature was similar to those of the class B specimens (fig. 1). Baker et al. (ref. 6) evaluated the plane-strain fracture toughness of 300M steel using round tensile specimens that were circumferentially notched and fatigued before testing. Their heat treatment consisted of austenitizing 0.5 hour at 1200 K (1700° F), oil quenching, and tempering as long as 4 hours at temperatures ranging from 477 K (400° F) to 866 K (1100° F) followed by air cooling. Contrary to the Bucher et al. results, Baker et al. found a monotonic increase of toughness with tempering temperature similar to the behavior of the class A specimens.

The effect of austenitizing temperature on the fracture toughness of the steel for selected tempering temperatures is shown in figure 4. The interesting feature is the dependence of the curve slopes on tempering temperature. Fracture toughness of as-quenched specimens and specimens tempered at 700 K (800° F) were relatively unaffected by austenitizing temperature. Toughness of the specimens tempered at 477 K (400° F) and 589 K (600° F) increased with austenitizing temperature, whereas specimens tempered at 811 K (1000° F) showed a decrease in toughness. This result suggests that the effects of austenitizing temperature and tempering temperature on toughness are interrelated.

Dual-austenitizing treatments.- Results from the fracture toughness tests of the dual-austenitizing treatments are shown in figure 5 alongside the results from the 1477 K (2200° F) single-austenitizing heat treatments. The similarity in the responses to these two treatments is evident.

Cryogenic tests.- Cryogenic mechanical properties were obtained to facilitate proof testing of landing gear components at low temperatures. Such tests should permit screening of flaws smaller than those identifiable by room-temperature proof testing. Both tension and fracture toughness tests were conducted at a series of cryogenic temperatures down to approximately 100 K (-280° F). The test results are plotted in figure 6. The response of tensile properties to the test temperatures was a gradual increase with decreasing temperature, whereas the toughness values decreased rapidly with decreasing temperature.

Microscopy

The microscopy results include quenching and tempering tests and fractography.

Quenched and tempered steels.- The austenitic grain size progressively increased with austenitizing temperature, as indicated in table III. Optical metallography also revealed that the martensitic plate size increased with

increasing austenitic grain size. Electron microscopy of the specimens revealed four significant features.

1. All class A specimens but no class B specimens contained evenly distributed undissolved ellipsoidal particles.

2. The martensitic substructure in all specimens consisted of laths and plates, and very few of the plates exhibited midrib twinning.

3. Autotempering was prevalent in the martensitic substructure.

4. Untransformed austenite was found at the lath and plate boundaries.

These structural features will be discussed in order.

The undissolved ellipsoidal particles, observed only in class A specimens, varied in size, with diameters ranging from 100 to 200 nanometers (1000 to 2000 angstroms). Their structure was identified by electron diffraction as face-centered cubic with a lattice parameter of 1.05 nanometers (10.5 angstroms). Unfortunately, this structure could not be correlated with any known and reasonable second-phase material. Figure 7 is a bright field image of a class A specimen in the as-quenched condition showing these undissolved particles. They were found inside the laths and plates and also at their boundaries. Specimens austenitized at 1255 K (1800° F) and above did not contain such particles, an indication that austenitizing at 1144 K (1600° F) places the steel either in the austenite plus "unidentified phase" region or barely within the austenitic region. Furthermore, from the dual-austenitizing treatment study it was discovered that the particles had not reprecipitated at 1144 K (1600° F) after 1 hour at 1477 K (2200° F). This indicates that the austenite phase boundary in 300M steel is probably slightly below 1144 K (1600° F), and 1 hour of austenitizing is insufficient to dissolve the particles.

The martensitic substructure consisted mainly of plates and laths and very few partly twinned plates. The morphological classifications of martensite already have been established by previous workers (refs. 8, 26, and 27) and need no amplification here. The extent of twinning was low (i.e., less than 5 percent of the martensitic plates were twinned) in both class A and class B specimens. The dissolution of the unidentified austenitic particles in class B specimens was not accompanied by any observable change in martensitic substructure. As previously mentioned, only the martensite plate size increased with increasing austenitic grain size.

Autotempering was extensive in class A and B specimens, and almost every plate and lath exhibited ϵ-carbides (autotempered carbides). Identification of these carbides was possible only by trace analysis. They were very fine compared to the previously mentioned ellipsoidal particles and may be seen faintly as thin platelets in figure 7. The size of these carbides was the same in both class A and class B specimens.

The presence of retained austenite in the as-quenched martensite has been reported by earlier workers (refs. 28 and 29). In the present study,

this retained austenite occurred in such low amounts that conventional X-ray diffraction techniques barely revealed its presence. The austenite, in most cases, outlined the lath and plate boundaries and occurred in thin platelets in some instances. The austenitic phase in the bright field image could not be discerned; however, selected area diffraction patterns supplemented by dark field studies confirmed its presence. Figure 8 contains bright and dark field images of a specimen quenched from 1144 K (1600° F). The reversal of contrast of austenite in a dark field was obtained by imaging the (200)γ reflections.[3] Extensive observation showed that the extent of the interlath and plate austenite was quite comparable in class A and B specimens, and no significant differences in the quantity of retained austenite could be detected.

Tempering of the steel produced analogous changes in microstructure in class A and B specimens. Tempering at 477 K (400° F) resulted in precipitation plus growth of the ϵ-carbide platelets in all the specimens, as typified by figure 9. Retained austenite was still present at the boundaries and could be readily observed in the structure. It appears that the onset of ϵ-carbide decomposition to cementite occurs at approximately 589 K (600° F). Tempering at 700 K (800° F) resulted in significant changes. The carbides were found to be cementite, and they were partly spheroidized. The most striking change was the decomposition of most of the retained austenite at the lath boundaries to cementite and, presumably, ferrite. Thus, a network of lath boundary carbides was found. Figure 10 contains the bright and dark field images of a class A specimen tempered at 700 K (800° F) showing discrete cementite precipitates at the lath boundaries. Isolated instances of retained austenite could also be found.

Tempering at 811 K (1000° F) spheroidized the cementite, and those spheroids were observed in the matrix and the boundaries as shown in figure 11. No evidence of recrystallization of martensite or rearrangement of dislocations was obtained. Retained austenite was totally absent.

The general response of 300M steel to tempering is in accordance with published results. The relatively high silicon content of this steel renders the tempering reaction sluggish (ref. 30). Hence, the carbides were predominantly ϵ-carbides, and the third stage of tempering is initiated at the relatively high tempering temperatures of 589 to 700 K (600° to 800° F). Thus, at low tempering temperatures of 477 to 589 K (400° to 600° F), ϵ-carbide is the dominant carbide in both class A and class B specimens.

Fractography.- Figure 12 contains a series of fractographs of the tested fracture toughness specimens quenched from 1144, 1255, and 1477 K (1600°, 1800°, and 2200° F). The fracture morphology is radically different between class A and class B specimens. Class A specimens showed a mixture of quasi-cleavage and dimpled rupture in proportions depending on the tempering temperature. No intergranular failure was observed at any tempering temperature.

---

[3]Circles scribed on the imaging screen of the microscope corresponding to the d-spacings of the (111)γ, (110)α, and (200)γ reflections greatly facilitated identification of austenite reflections in the diffraction pattern.

Class B specimens also failed by a mixture of quasi-cleavage and dimpled rupture in the tempering range of 477 to 589 K (400° to 600° F) but with somewhat less quasi-cleavage than class A specimens. In sharp contrast, class B specimens tempered at and above 700 K (800° F) failed by an intergranular mode. In each case, the fractographs were compared with the optical micrographs to verify that intergranular failure was indeed along the prior austenite grain boundaries.

A limited number of high-resolution fractographs were prepared by gold coating the fracture surfaces. These were examined for evidence of the 100- to 200-nanometer (1000 to 2000 angstrom) particles that had been observed in class A samples by TEM. Particles of the proper size were found concentrated on the quasi-cleavage regions of class A specimens (fig. 13). They were never found on the dimpled rupture regions. Similar but smaller (50-nanometer (500 angstrom)) particles were found on the fracture surface of a sample austenitized at 1200 K (1700° F). These particles were also localized in the quasi-cleavage region. Only one quasi-cleavage region was found on the class B sample observed, and it also had 50-nanometer (500 angstrom) particles. This sample had been austenitized at 1255 K (1800° F) and tempered at 589 K (600° F). The fact that no particles were seen in TEM must have been a result of the smaller area available for observation. The fracture surface studied was approximately 2000 times larger than a typical TEM region.

DISCUSSION

Significant Observations

The most significant observations from the present research are the following.

1. Tempering in the range of 477 to 589 K (400° to 600° F) produced substantially higher toughness in class B specimens than in class A specimens. Conversely, tempering at 700 to 811 K (800° to 1000° F) produced the opposite effect. Tempering at 700 K (800° F) produced a minimum in the curves of toughness as a function of tempering temperature for class B specimens.

2. The microstructure of both classes as determined by transmission electron microscopy was qualitatively alike. After tempering at temperatures below 700 K (800° F), the structure consisted of a uniform dispersion of ε-carbide in lightly twinned martensite with small amounts of austenite in the lath and plate boundaries. After tempering at or above 700 K (800° F), the ε-carbide transformed to cementite and the retained austenite transformed to ferrite and cementite. However, the following differences were noted between class A and class B specimens.

   a. Class A samples were found to have undissolved ellipsoidal particles. These appeared to be completely dissolved in the class B specimens. Dual-austenitizing treatment from 1477 to 1144 K (2200° to 1600° F) did not cause particles to reprecipitate.

b. The quasi-cleavage regions of fracture surfaces of class A samples contained high concentrations of particles similar in appearance and size to the undissolved ellipsoidal particles.

c. Austenite grain size increased with increasing austenitizing temperature. As a consequence, the martensite plates were also larger at higher austenitizing temperatures.

3. Fracture surfaces were ductile and transgranular except for class B specimens tempered at or above 700 K (800° F). These failed by intergranular cleavage.

As-Quenched Structure

Some recent studies (refs. 23 and 31) indicate that use of a higher austenitizing temperature followed by oil quenching, but no subsequent tempering, provides high toughness in some commercial steels. The present work cannot confirm these results for 300M steel. In fact, excessive brittleness of all the as-quenched specimens posed great difficulty in avoiding premature failure of the fracture toughness specimens during the fatigue precracking phase before testing. Optical and transmission electron microscopy results have shown that the as-quenched structure is uniformly martensitic with small amounts of austenite at the lath and plate boundaries. No other transformation occurs at the grain boundaries during quenching. Because all the as-quenched fracture specimens showed transgranular failure, it follows that austenite at the lath and plate boundaries does not lessen brittle failure in the as-quenched condition. The transgranular nature of the as-quenched fracture toughness specimen also rules out any possibility of impurity segregation at the grain boundaries as suggested by McMahon (ref. 32), who observed intergranular failure in as-quenched specimens. Thus, the austenite grain size has no effect on the toughness of the as-quenched steel.

Quenched and Tempered Structures

The discussion of quenched and tempered structures includes specimens subjected to tempering temperatures below 700 K (800° F) and specimens subjected to tempering temperatures of 700 K (800° F) and higher.

Tempering temperatures below 700 K (800° F).- The effect on toughness of microstructural changes accompanying austenitizing temperatures can be evaluated from table III and figures 1 and 4. Increase of austenitizing temperature caused an increase in austenitic grain size and, between 1144 K (1600° F) and 1255 K (1800° F), resulted in dissolution of the particles discussed previously. Specimens tempered at 477 K (400° F) and 589 K (600° F) increased in toughness with an increase in austenitizing temperature; the most pronounced improvement occurred concurrently with the dissolution of the second-phase particles. Thus, it appears possible that the second-phase particles facilitated crack propagation in the tempered class A specimens, and their removal resulted in higher toughness. Improvement in toughness with increasing austenite grain size has been noted earlier (refs. 23 and 31), and some of the

increase in toughness with increasing austenitizing temperature can be attributed to this effect. As-quenched toughness is relatively unaffected by austenitizing temperature.

The results of the reported study show that twins in martensite are not sufficient to cause low toughness. Both class A and class B specimens possess comparable but low amounts of twins, and the toughness responses are widely different. Furthermore, a low level of twinning does not promote toughness of the steel either in the as-quenched condition or in the quenched and tempered condition. The structure that produced the highest toughness values consisted of uniform ε-carbide precipitates in a martensitic matrix. Reports by Lindborg and Averbach (ref. 33) and Liu (ref. 15) showed that coherency strain associated with ε-carbide is fairly isotropic and hence does not retard the crack growth as much as the cementite precipitate does in a bainitic structure. The present results show that the toughness of the martensitic structure with ε-carbide precipitates is high in the absence of undissolved precipitate particles. The question that remains unanswered relates to the brittleness of the untempered martensitic structure. The as-quenched microstructure consisting of a fine dispersion of autotempered ε-carbide in a martensitic matrix was brittle. Tempering at 477 K (400° F) caused only the ε-carbide precipitates to grow, but the toughness of the steel improved appreciably. The reason for this behavior is still unclear. It can be speculated that the ε-carbide formed during quenching depletes the carbon locally and thus renders the carbide/matrix interface weak. Tempering at 477 K (400° F) homogenizes the carbon and leaves behind no such weak interfaces.

Tempering temperatures of 700 K (800° F) and above.- The low toughness of class B specimens after tempering at 700 K (800° F) or higher can possibly be explained in the same manner as "350° C embrittlement" (refs. 32 and 34 to 37). The observed decohesion along prior austentite grain boundaries clearly suggests that the micromechanism (or micromechanisms) initiating the failure is definitely at the grain boundary rather than in the matrix. The current understanding of the embrittlement involves a dual mechanism. During austenitization, solute alloying elements segregate at the austenite grain boundaries. During subsequent tempering at 700 K or higher, impurity elements such as phosphorus and antimony segregate to the prior austenite boundaries and thereby produce a structurally weakened region. Previous reports (refs. 36 and 38) that the severity of embrittlement is accentuated by large austenitic grains are in accordance with the present results. Large grain size is equivalent to small grain boundary area. Therefore, for a given level of impurity elements, the larger the grain size, the more effectively will these impurities be capable of saturating the grain boundary regions. The steel used in the present investigation has a lower phosphorus content than steels used earlier (refs. 31 to 35), and the class A specimens with austenite grain size 8 were practically free of this embrittlement. A cutoff grain size for embrittlement thus appears to exist in 300M steel, and it is somewhere between ASTM grain sizes 5 and 8. This argument is supported by the fact that the toughness response of the step-quenched specimens was strikingly similar to that of specimens quenched directly from 1477 K (2200° F). This result indicates that the austenitic grain size rather than some indirect effect from the austenitizing treatment governs the potential for embrittlement. Similar observations were made by Woodfine (ref. 38).

SUPPLEMENTARY EXPERIMENTS

Because the ellipsoidal particles that seemed responsible for reducing toughness in the class A heat treatments appeared to be completely dissolved after 1 hour at 1255 K (1800° F), additional studies were performed in the austenitizing region between the class A and the class B treatments. Samples were austenitized at a variety of times and temperatures and examined by TEM to determine the lowest austenitizing temperature that would dissolve the particles. Austenitizing times of as long as 8 hours at 1144 K (1600° F) did not dissolve the particles, nor did 1 hour at 1172 K (1650° F). However, 1 hour at 1200 K (1700° F) eliminated most of the precipitates, and this time and this temperature were selected for supplementary plane-strain fracture toughness determinations. Toughness was evaluated as before using the 0.0127-meter (0.5 inch) sample thickness. The results in figure 14 show that this heat treatment resulted in behavior which was intermediate between class A and class B material. The data scatter was greater than expected, and no reason could be found to explain it from either the test procedures or the heat treatment. Possibly, the incidence of undissolved second-phase particles was critically sensitive to composition and varied between samples enough to cause the observed wide scatter in toughness. Times longer than 1 hour at the austenitizing temperature or a slightly higher temperature might have reduced this scatter in toughness.

SELECTION OF HEAT TREATMENTS

From the present results, one can select heat treatments that optimize yield strength and toughness. Figure 15 shows one way in which this may be done. Here, the fracture toughness has been plotted against the yield strength for all the data available from the 0.0127-meter (0.5 inch) tests. The crosshatched region was arbitrarily drawn for illustrative purposes to show those heat treatments that would produce yield strength of at least 1550 MN/m^2 (225 ksi) and toughness of at least 82.4 $MN/m^{3/2}$ (75 ksi$\sqrt{in.}$). One should note that several heat treatments fall within the hatched region, but the conventionally recommended treatment does not. One can also see from this figure that high strength does not necessarily imply low toughness nor the converse. From earlier discussion in this paper, it could be inferred that the contribution of second-phase-particle dissolution to toughness is the dominant factor. However, advantage could be taken of the contribution of the grain size to toughness, and it is recommended that 300M steel generally be austenitized at the highest possible temperature. However, one should be aware of several problems attending the use of high austenitizing temperatures, elaborated by Ritchie and Knott (ref. 31). Not all large structures can be easily fast quenched from temperatures higher than 1373 K (2012° F) without the possible occurrence of quench cracking from thermal stress. Furthermore, if the cooling rate is excessively slow, the improvement in toughness is greatly reduced. Finally, if the steels are austenitized at a temperature high enough to dissolve sulfides and if the quenching rate is insufficient to suppress their precipitation on austenite grain boundaries, then toughness and resistance to fatigue growth will be significantly reduced. This last problem has

been termed "overheating." Because of this last consideration, Ritchie and Knott recommended that the austenitizing temperature not exceed 1423 to 1473 K (2101° to 2192° F). Tempering above 589 K (600° F) should be avoided since larger grain sizes aggravate the intergranular failure.

SUMMARY AND RECOMMENDATIONS

The tensile strength and the plane-strain fracture toughness resulting from a variety of heat treatments were evaluated. Measurements taken over a wide range of austenitizing and tempering temperatures showed that the conventional austenitizing temperature of 1144 K (1600° F) results in a penalty in toughness performance. Results of microstructural studies performed in parallel with the mechanical tests indicate that the lower toughness was probably caused by a second-phase precipitate particle which does not dissolve at 1144 K (1600° F) but appears to dissolve readily at 1255 K (1800° F) and above.

In cases requiring the optimum in both strength and toughness, it is recommended that austenitization be performed at 1255 K (1800° F) or higher and that tempering be performed in the range 477 to 589 K (400° to 600° F). Limited supplementary tests indicate that austenitizing at 1200 K (1700° F) improves toughness substantially, but with some scatter in performance. It is also recommended that alloy manufacturers investigate modifications to the composition or processing of 300M steel (e.g., possibly by normalizing at 1266 K (1800° F)) to eliminate the second-phase particles seen here. This refinement would improve toughness without requiring austenitization at excessive temperatures.

Lyndon B. Johnson Space Center
National Aeronautics and Space Administration
Houston, Texas, May 22, 1978
953-36-00-00-72

REFERENCES

1. Huang, Der-Hung; and Thomas, G.: Structure and Mechanical Properties of Tempered Martensite and Lower Bainite in Fe-Ni-Mn-C Steels. Met. Trans., vol. 2, no. 6, June 1971, pp. 1587-1598.

2. Zackay, V. F.; Parker, E. R.; Goolsby, R. D.; and Wood, W. E.: Untempered Ultra-High Strength Steels of High Fracture Toughness. Nature Phys. Sci., vol. 236, no. 68, 1972, pp. 108-109.

3. Das, S. K.; and Thomas, G.: Structure and Mechanical Properties of Fe-Ni-Co-C Steels. American Soc. Metals Trans., vol. 62, 1969, pp. 659-676.

4. Thomas, G.; Schmatz, D.; and Gerberich, W.: Structure and Strength of Some Ausformed Steels. High Strength Materials - Proceedings of the Second Berkeley International Materials Conference, Victor F. Zackay, ed., J. Wiley and Sons, 1965, pp. 251-326.

5. Banerjee, B. R.: Embrittlement of High-Strength Tempered Alloy Martensites. J. Iron & Steel Inst., vol. 203, pt. 2, Feb. 1965, pp. 166-174.

6. Baker, A. J.; Lauta, F. J.; and Wei, R. P.: Relationship Between Microstructure and Toughness in Quenched and Tempered Ultra-High-Strength Steels. Structure and Properties of Ultrahigh Strength Steels, American Soc. Testing Mater. spec. tech. pub. 370, 1965, pp. 3-22; discussion, pp. 23-29.

7. Page, E. W.; Manganon, P., Jr.; Thomas, G; and Zackay, V. F.: Structure and Properties of Dynamically Strain Aged Fe-Cr-C and Fe-Mo-C Alloys. American Soc. Metals Trans., vol. 62, 1969, pp. 45-54.

8. Kelly, P. M.; and Nutting, J.: Strengthening Mechanisms in Martensite. Physical Properties of Martensite and Bainite, Iron & Steel Inst. spec. rep. 93, 1965, pp. 166-178.

9. Low, John R., Jr.: Effects of Microstructure on Fracture Toughness of High-Strength Alloys. Eng. Fract. Mech., vol. 1, no. 1, June 1968, pp. 47-53.

10. Pellissier, G. E.: Effects of Microstructure on Fracture Toughness of Ultrahigh-Strength Steels. Eng. Fract. Mech., vol. 1, no. 1, June 1968, pp. 55-75.

11. Banerjee, Bani R.: Fracture Micromechanics in High-Strength Steels. Structure and Properties of Ultrahigh Strength Steels, American Soc. Testing Mater. spec. tech. pub. 370, 1968, pp. 94-116; discussion, pp. 116-120.

12. Hahn, G. T.; and Rosenfield, A. R.: Sources of Fracture Toughness: The Relation Between K_{Ic} and the Ordinary Tensile Properties of Metals. Applications-Related Phenomena in Titanium and Its Alloys, American Soc. Testing Mater. spec. tech. pub. 432, 1968, pp. 5-32.

13. Liu, Y. H.: Correlation of Microstructures With Toughness in HP 9-4-45 Lower Bainite and Tempered Martensite. American Soc. Metals Trans., vol. 62, 1969, pp. 55-63.

14. Vishnevsky, C.; and Steigerwald, E. A.: Influence of Alloying Elements on the Low-Temperature Toughness of Martensite High-Strength Steels. American Soc. Metals Trans., vol. 62, 1969, pp. 305-317.

15. Liu, Y. H.: Eff of Carbides on Fracture Path in Lower Bainite and Tempered Martensite. American Soc. Metals Trans., vol. 62, 1969, pp. 544-547.

16. Kula, E. B; and Anctil, A. A.: Tempered Martensite Embrittlement and Fracture Toughness in SAE 4340 Steel. J. Mater., vol. 4, no. 4, Dec. 1969, pp. 817-841.

17. Lement, B. S.; Averbach, B. L.; and Cohen, Morris: Microstructural Changes on Tempering Iron-Carbon Alloys. American Soc. Metals Trans., vol. 46, 1954, pp. 851-877.

18. Pascover, J. S.; and Matas, S. J.: Relationships Between Structure and Properties in the 9Ni-4Co Alloy System. Structure and Properties of Ultrahigh-Strength Steels, American. Soc. Testing Mater. spec. tech. pub. 370, 1965, pp. 30-44; discussion, pp. 45-46.

19. Klingler, L. J.; Barnett, W. J.; Frohmberg, R. P.; and Troiano, A. R.: The Embrittlement of Alloy Steel at High Strength Levels. American Soc. Metals Trans., vol. 46, 1954, pp. 1557-1598.

20. Ritchie, Robert O.; Francis, Benjamin; and Server, William L.: Evaluation of Toughness in AISI 4340 Alloy Steel Austenitized at Low and High Temperatures. Met. Trans., vol. 7A, no. 6, June 1976, pp. 831-838.

21. Pendleberry, S. L.; Simenz, R. F.; and Walker, R. K.: Fracture Toughness and Crack Propagation of 300M Steel. Lockheed-California Co. report to Federal Aviation Administration, rep. no. FAA-DS-68-18, 1968.

22. Bucher, J. H.; Powell, G. W.; and Spretnak, J. W.: A Micro-Fractographic Analysis of Fracture Surfaces in Some Ultra-High-Strength Steels. Applications of Fracture Toughness Parameters to Structural Metals, Metallurgical Society of AIME Proceedings, Herman D. Greenberg, ed., Gordon and Breach (New York), 1966, pp. 323-371.

23. Wood, W. E.; Parker, E. R.; and Zackay, V. F.: Investigation of Metallurgical Factors Which Affect the Fracture Toughness of Ultra High Strength Steels. Lawrence Berkeley Laboratory rep. no. LB-1474, 1973.

24. Wood, William E.: Effect of Heat Treatment on the Fracture Toughness of Low Alloy Steels. Eng. Fract. Mech., vol. 7, no. 2, 1975, pp. 219-234.

25. Youngblood, J. L.: Preparation of Samples for Transmission Electron Microscopy by Illuminated Jet Polishing. American Soc. Metals Trans., vol. 62, 1969, pp. 1019-1023.

26. Thomas, Gareth: Electron Microscopy Investigations of Ferrous Martensites. Met. Trans., vol. 2, no. 9, Sept. 1971, pp. 2373-2385.

27. Kelly, P. M.; and Nutting, J.: Morphology of Martensite. J. Iron & Steel Inst., vol. 197, pt. 3, Mar. 1961, pp. 199-211.

28. McMahon, John A.; and Thomas, Gareth: Development of Economical, Tough, Ultra-High Strength Iron-Chromium-Carbon Steels. Microstruct. Des. Alloys, Proc. 3rd International Conference on Strength of Metals and Alloys, Vol. 1, Inst. Metals/Iron & Steel Inst., 1973, pp. 180-184.

29. Lai, G. Y.; Wood, W. E.; et al.: The Effect of Austenitizing Temperature on the Microsructure and Mechanical Properties of As-Quenched 4340 Steel. Met. Trans., vol. 5, no. 7, July 1974, pp. 1663-1670.

30. Shih, C. H.; Averbach, B. L.; and Cohen, Morris: Some Effects of Silicon on the Mechanical Properties of High-Strength Steels. American Soc. Metals Trans., vol. 48, 1956, pp. 86-110.

31. Ritchie, R. O.; and Knott, J. F.: On the Influence of High Austenitizing Temperatures and "Overheating" on Fracture and Fatigue Crack Propagation in a Low Alloy Steel. Met. Trans., vol. 5, Mar. 1974, pp. 782-785.

32. McMahon, C. J., Jr.: Temper Brittleness - An Interpretive Review. Temper Embrittlement in Steel, American Soc. Testing Mater. spec. tech. pub. 407, 1968, pp. 127-167.

33. Lindborg, U. H.; and Averbach, B. L.: Crystallographic Aspects of Fracture in Martensite. Acta Met., vol. 14, Nov. 1966, pp. 1583-1593.

34. Schwartzbart, H.; and Sheehan, J. P.: How Carbon Content Affects Impact Properties. Iron Age, vol. 178, no. 6, Aug. 9, 1956, pp. 85-89.

35. Capus, J. M.; and Mayer, G.: Influence of Trace Elements on Embrittlement in Low-Alloy Steels. Metallurgia, vol. 62, no. 372, Oct. 1960, pp. 133-138.

36. Capus, J. M.: Austenite Grain Size and Temper Brittleness. J. Iron & Steel Inst., vol. 200, pt. 11, Nov. 1962, pp. 922-927.

37. Capus, J. M.: The Mechanism of Temper Brittleness. Temper Embrittlement in Steel, American Soc. Testing Mater. spec. tech. pub. 407, 1968, pp. 3-19.

38. Woodfine, B. C.: Temper-Brittleness: Critical Review of Literature. J. Iron & Steel Inst., vol. 173, pt. 3, Mar. 1953, pp. 229-240.

TABLE I.- MECHANICAL PROPERTIES OF 0.0127-METER (0.5 INCH) THICK BAR STOCK OF QUENCHED AND TEMPERED 300M STEEL

Austenitizing temperature, K (°F)	Tempering temperature, K (°F)	Yield strength, MN/m^2 (ksi)	Ultimate strength, MN/m^2 (ksi)	Plane-strain fracture toughness, $MN/m^{3/2}$ (ksi$\sqrt{in.}$)
1144 (1600)	As quenched	1364 (198)	2273 (330)	39.5 (36)
	477 (400)	1516 (220)	1956 (284)	58.2 (53)
	560 (550)	1584 (230)	1874 (272)	69.2 (63)
	589 (600)	1624 (236)	1894 (275)	62.6 (57)
	700 (800)	1378 (200)	1701 (247)	65.9 (60)
	811 (1000)	1364 (198)	1529 (222)	97.8 (89)
1255 (1800)	As quenched	1343 (195)	2129 (309)	47.2 (43)
	477 (400)	1564 (227)	1998 (290)	82.4 (75)
	589 (600)	1619 (235)	1929 (280)	78.0 (71)
	700 (800)	1612 (234)	1736 (252)	61.5 (56)
	811 (1000)	1398 (203)	1591 (231)	81.3 (74)
1366 (2000)	As quenched	1267 (184)	2301 (334)	45.0 (41)
	477 (400)	1522 (221)	1984 (288)	87.9 (80)
	589 (600)	1619 (235)	1929 (280)	84.6 (77)
	700 (800)	1577 (229)	1839 (267)	54.9 (50)
	811 (1000)	1398 (203)	1564 (227)	68.1 (62)
1477 (2200)	As quenched	1322 (192)	2239 (325)	48.3 (44)
	477 (400)	1550 (225)	1963 (285)	90.1 (82)
	589 (600)	1591 (231)	1881 (278)	86.8 (79)
	700 (800)	1564 (227)	1667 (242)	58.2 (53)
	811 (1000)	1433 (208)	1626 (236)	62.6 (57)

TABLE II.- MECHANICAL PROPERTIES OF 0.0254-METER (1.0 INCH) THICK BAR STOCK OF QUENCHED AND TEMPERED 300M STEEL

Austenitizing temperature, K (°F)	Tempering temperature, K (°F)	Yield strength, MN/m^2 (ksi)	Ultimate strength, MN/m^2 (ksi)	Plane-strain fracture toughness, $MN/m^{3/2}$ (ksi$\sqrt{in.}$)
1144 (1600)	As quenched	(a)	(a)	49 (45)
	477 (400)	1399 (203)	1977 (287)	58 (53)
	560 (550)	1564 (227)	1860 (270)	66 (60)
	589 (600)	1598 (232)	1840 (267)	62 (56)
	700 (800)	1399 (203)	1723 (250)	62 (56)
	811 (1000)	1357 (197)	1550 (225)	99 (90)
1255 (1800)	As quenched	1247 (181)	2232 (324)	49 (45)
	477 (400)	1454 (211)	1971 (286)	75 (68)
	589 (600)	1550 (225)	1929 (280)	78 (71)
	700 (800)	1378 (200)	1723 (250)	56 (51)
	811 (1000)	1406 (204)	1578 (229)	78 (71)
1366 (2000)	As quenched	1261 (183)	2067 (300)	45 (41)
	477 (400)	1309 (190)	2026 (294)	80 (73)
	589 (600)	1530 (222)	1888 (274)	77 (70)
	700 (800)	1399 (203)	1743 (253)	56 (51)
	811 (1000)	1378 (200)	1516 (220)	66 (60)
1477 (2200)	As quenched	1178 (171)		52 (47)
	477 (400)	1309 (190)	2019 (293)	86 (78)
	589 (600)	1502 (218)	1860 (270)	81 (74)
	700 (800)	1543 (224)	1860 (270)	56 (51)
	811 (1000)	1378 (200)	1509 (219)	62 (56)

[a]Specimen failed before test.

TABLE III.- EFFECT OF AUSTENITIZING TREATMENT ON AUSTENITIC GRAIN SIZE

Austenitizing temperature, K (°F)	ASTM grain size
1144 (1600)	8
1255 (1800)	5
1366 (2000)	3.5
1477 (2200)	1

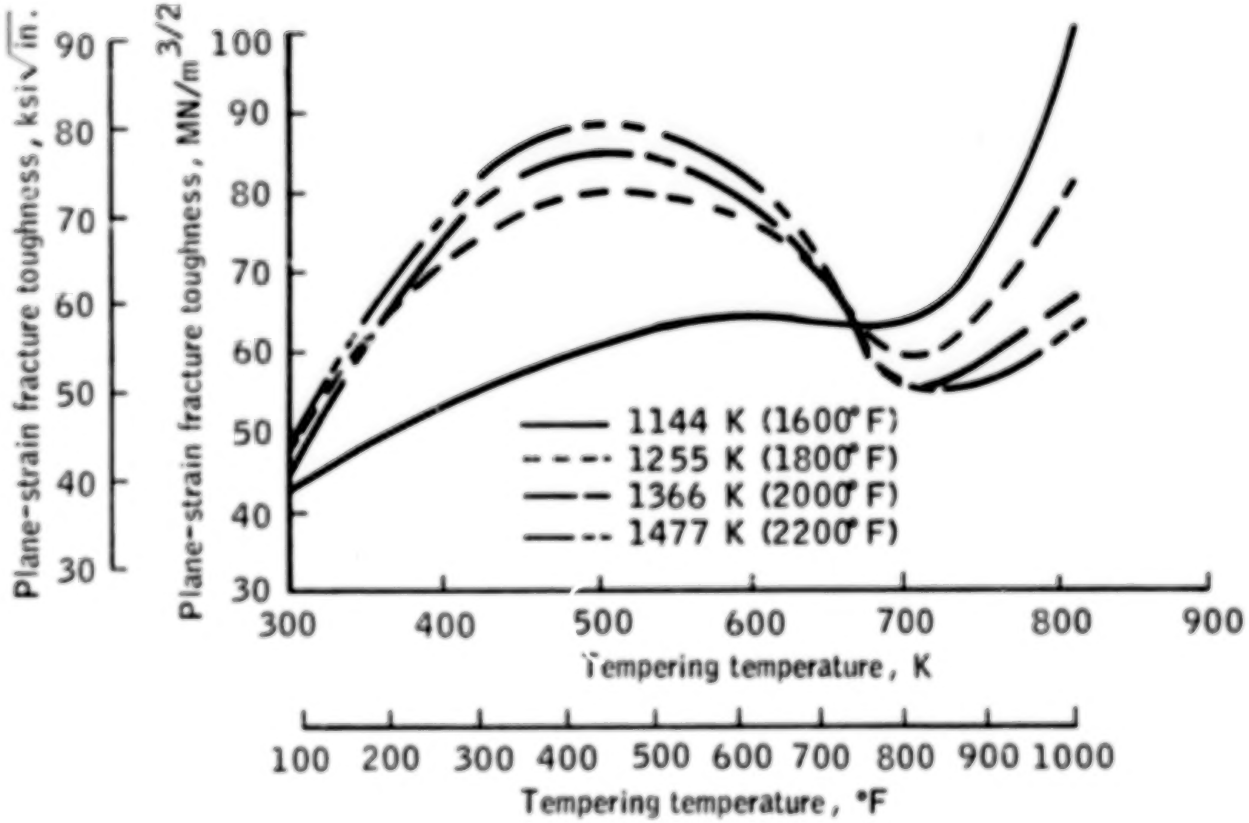

Figure 1.- Effect of tempering temperature on the plane-strain fracture toughness of 300M steel at four austenitizing temperatures.

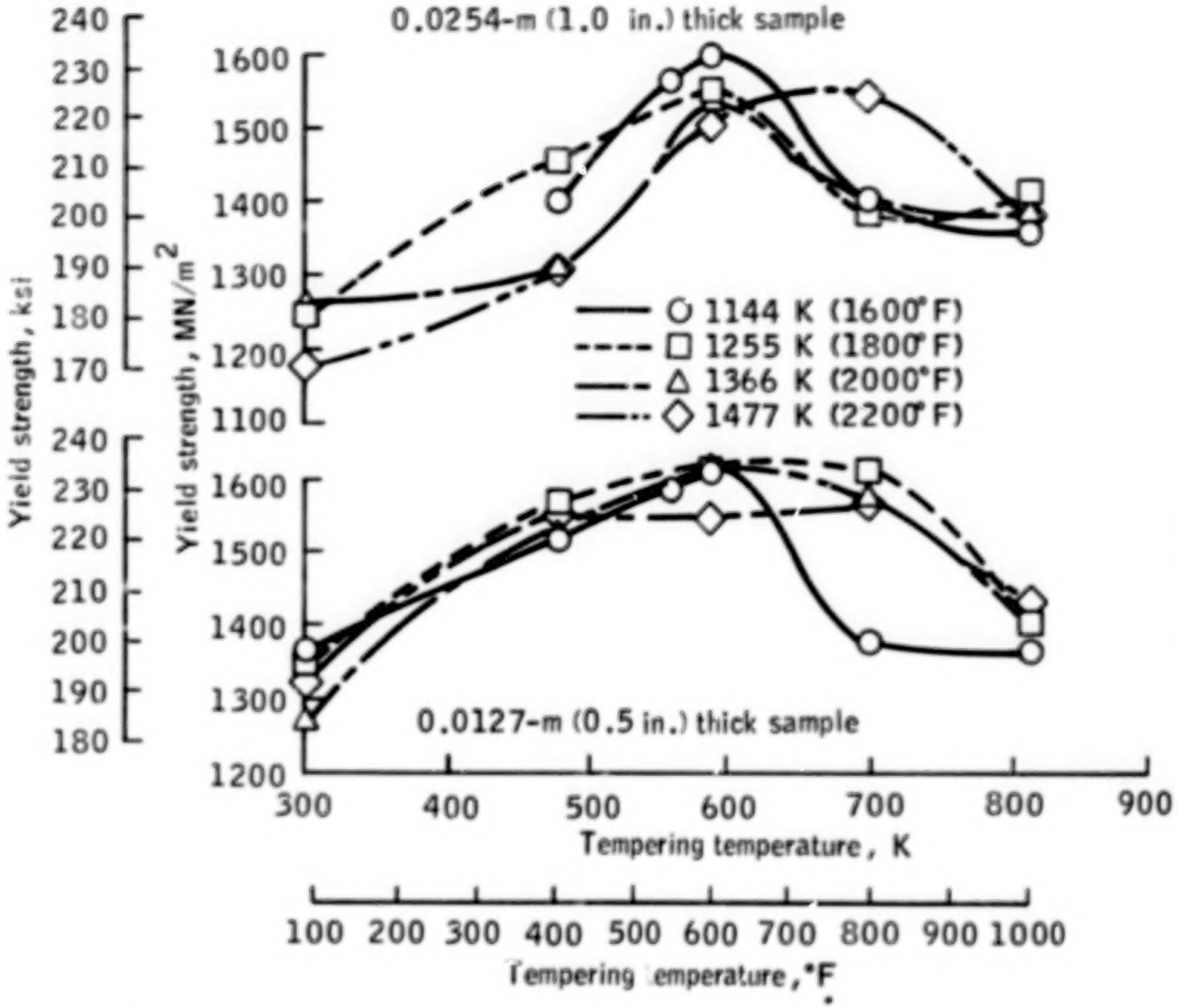

Figure 2.- Effect of tempering temperature on the 0.2-percent tensile yield strength of 300M steel at four austenitizing temperatures.

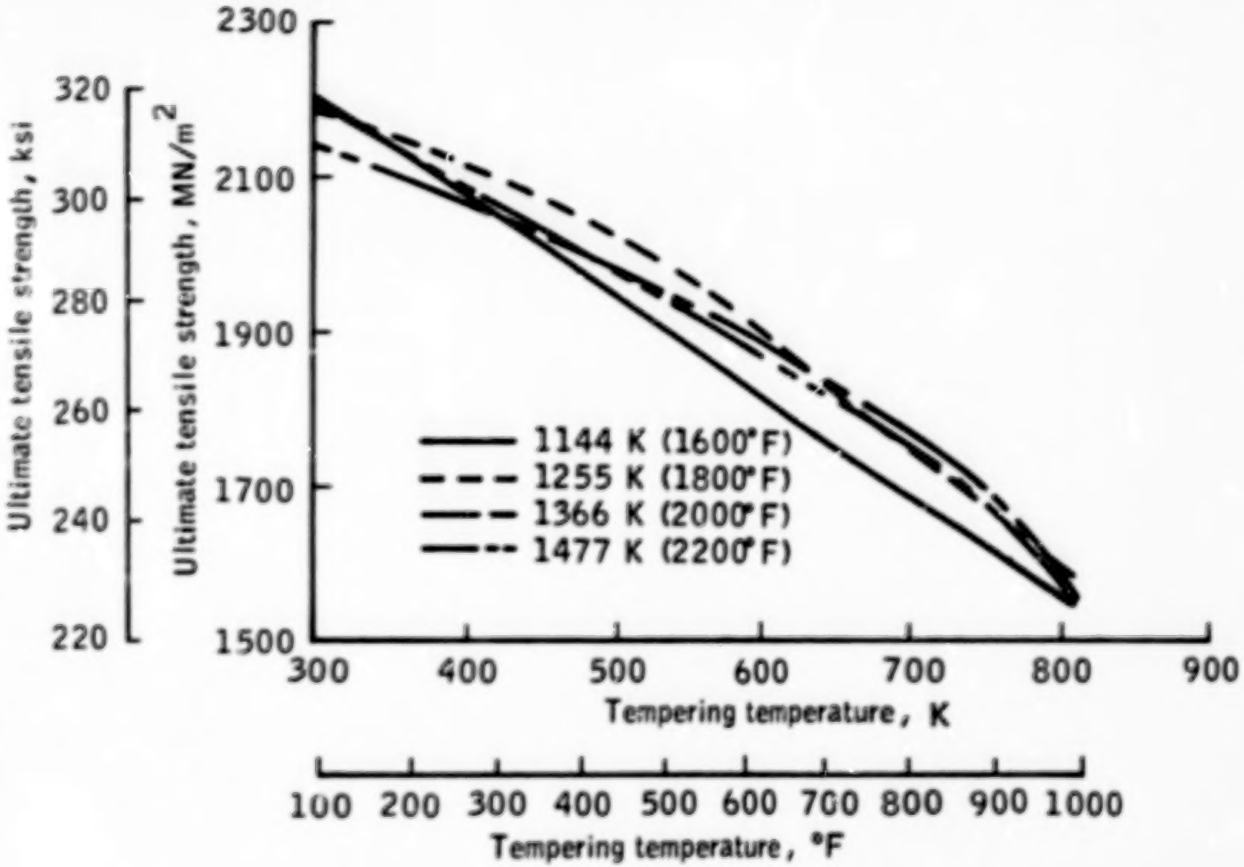

Figure 3.- Effect of tempering temperature on the ultimate tensile strength of 300M steel at four austenitizing temperatures.

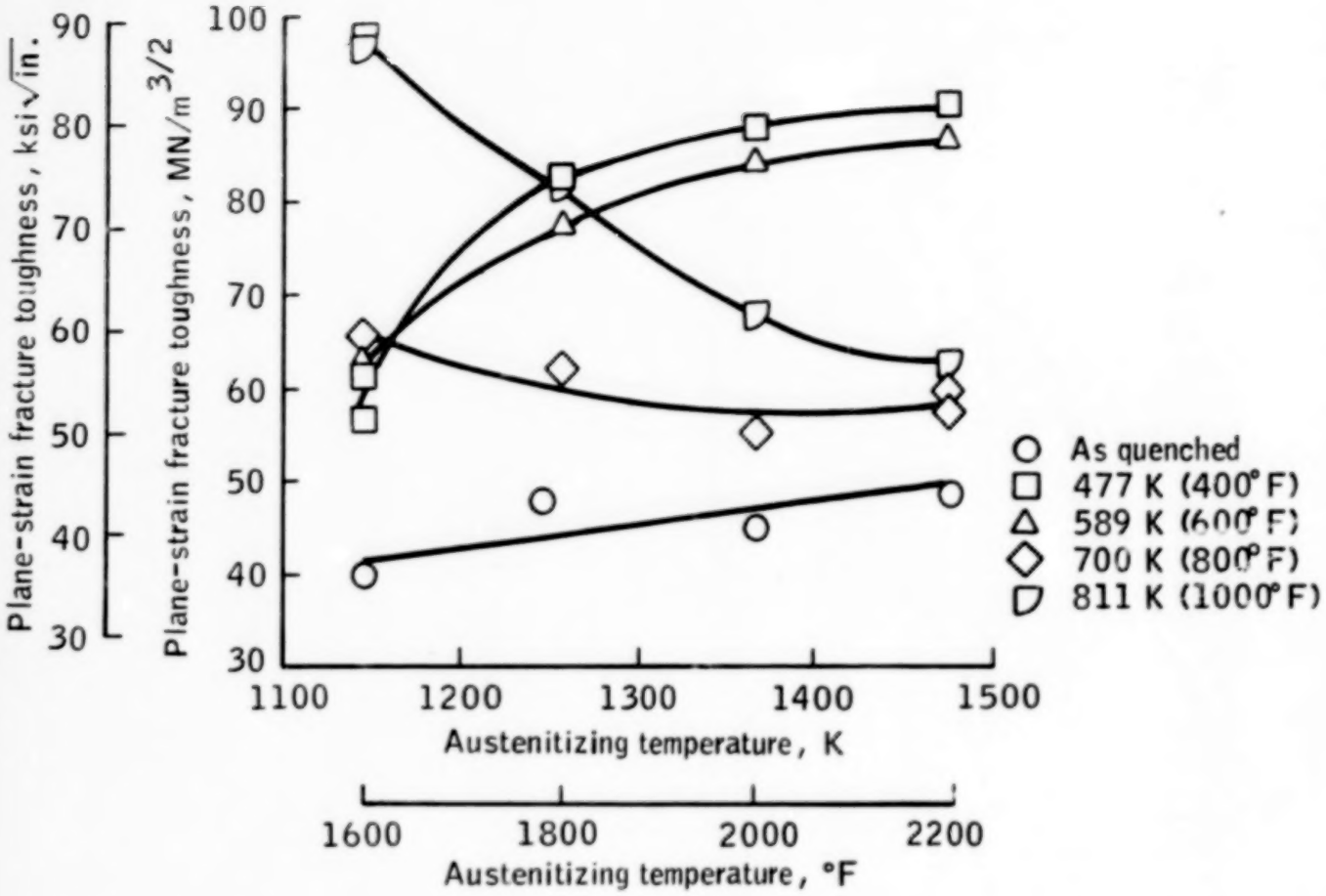

Figure 4.- Effect of austenitizing temperature on the plane-strain fracture toughness of 300M steel at five tempering temperatures. The sample thickness was 0.0127 meter (0.5 inch).

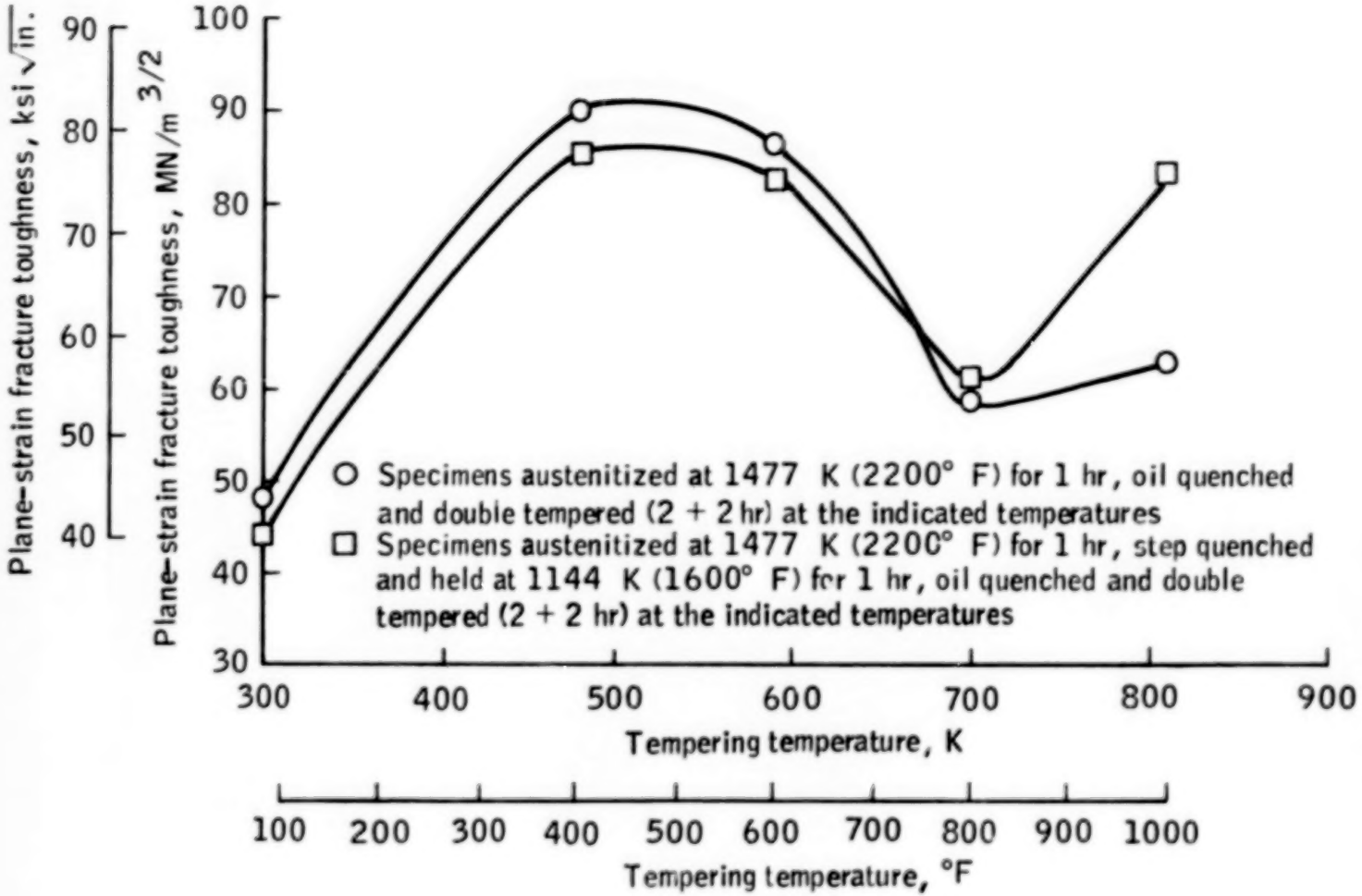

Figure 5.- Comparison of the effects of tempering on the plane-strain fracture toughness of specimens handled in two ways: (1) quenched directly from 1477 K (2200° F) to room temperature and (2) step-quenched from 1477 K (2200° F) to 1144 K (1600° F) to room temperature.

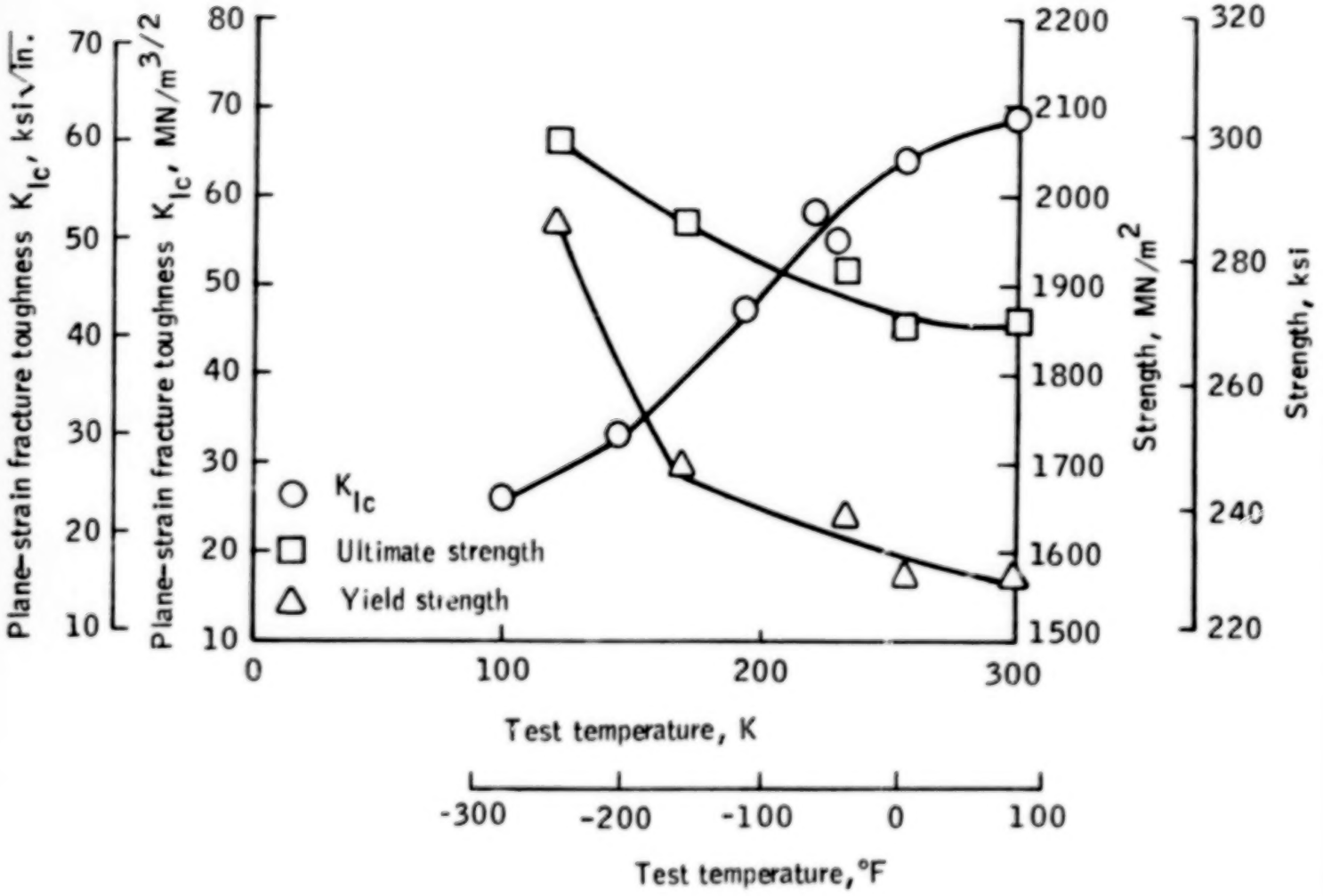

Figure 6.- Effect of cryogenic temperature on the plane-strain fracture toughness, the 0.2-percent tensile yield strength, and the ultimate tensile strength of 300M steel.

Figure 7.- Bright field image of 300M steel specimen austenitized at 1144 K (1600° F) and quenched to room temperature. Undissolved particles are indicated by arrows.

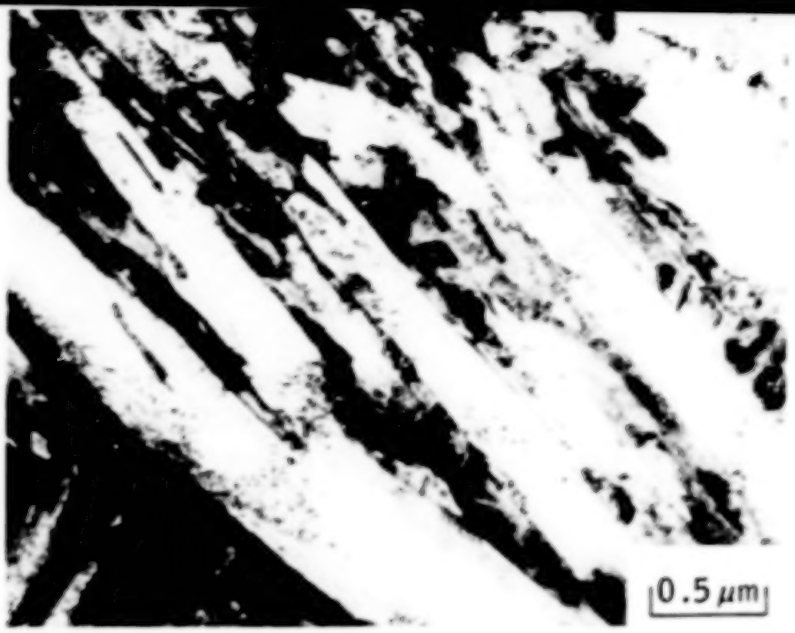

(a) Bright field image showing martensitic substructure. Autotempering is evident in the laths. An undissolved particle is indicated by arrow.

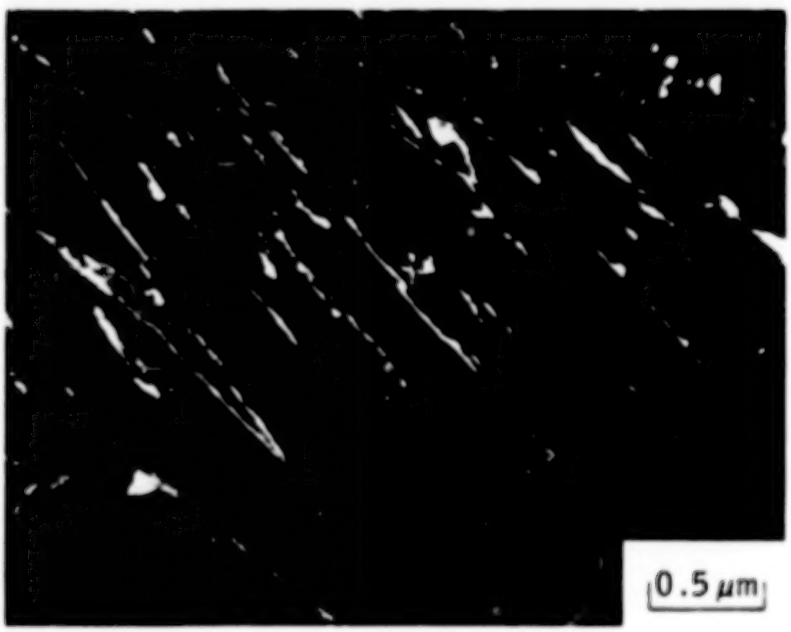

(b) Dark field image of a (200)γ reflection reverses the contrast of the austenite at the interlath boundaries.

Figure 8.- Bright field and dark field images of 300M steel specimen austenitized and quenched from 1144 K (1600° F).

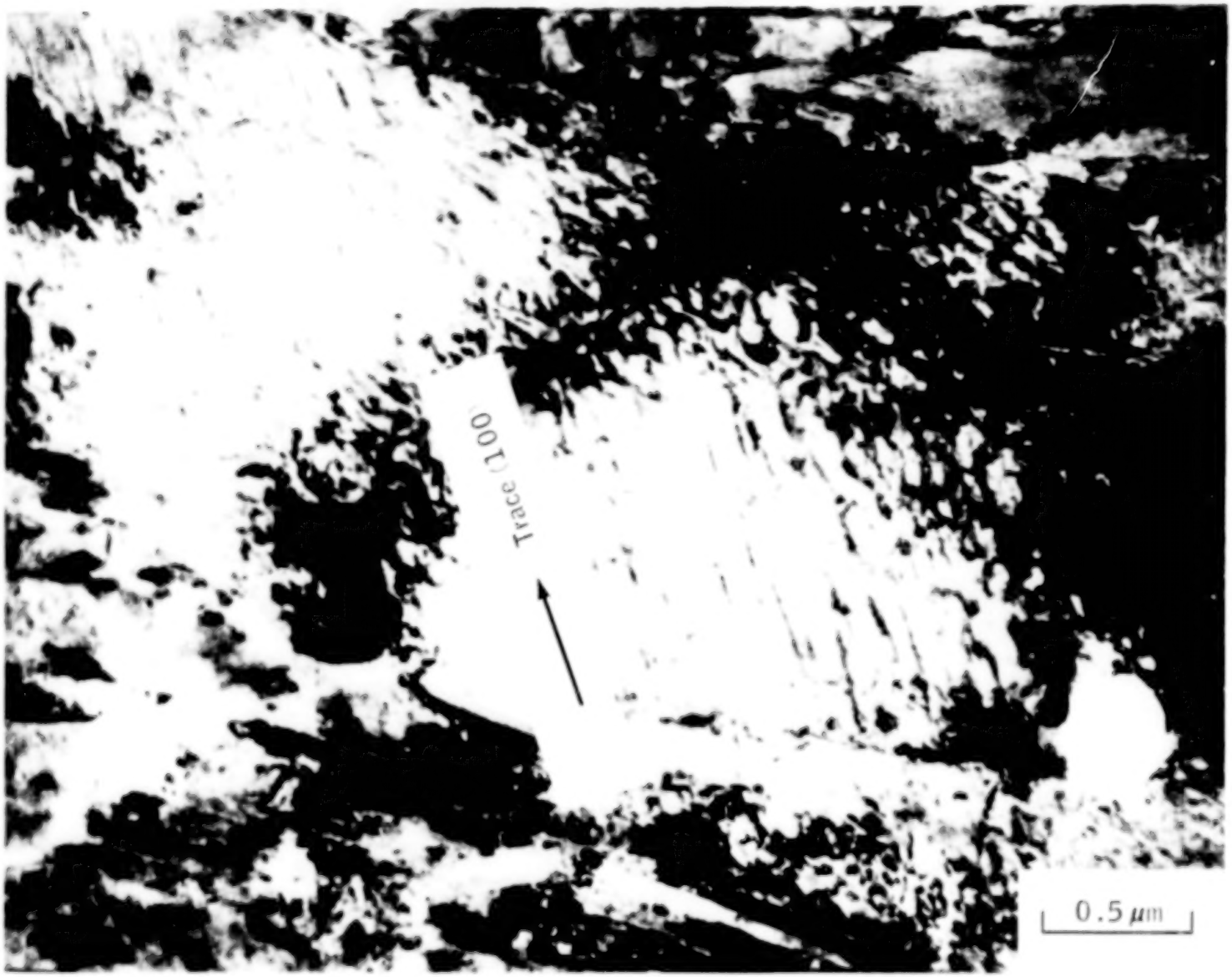

Figure 9.- Bright field image of 300M steel specimen austenitized at 1144 K (1600° F) and quenched to room temperature. Autotempered ε-carbide is shown in a martensitic plate.

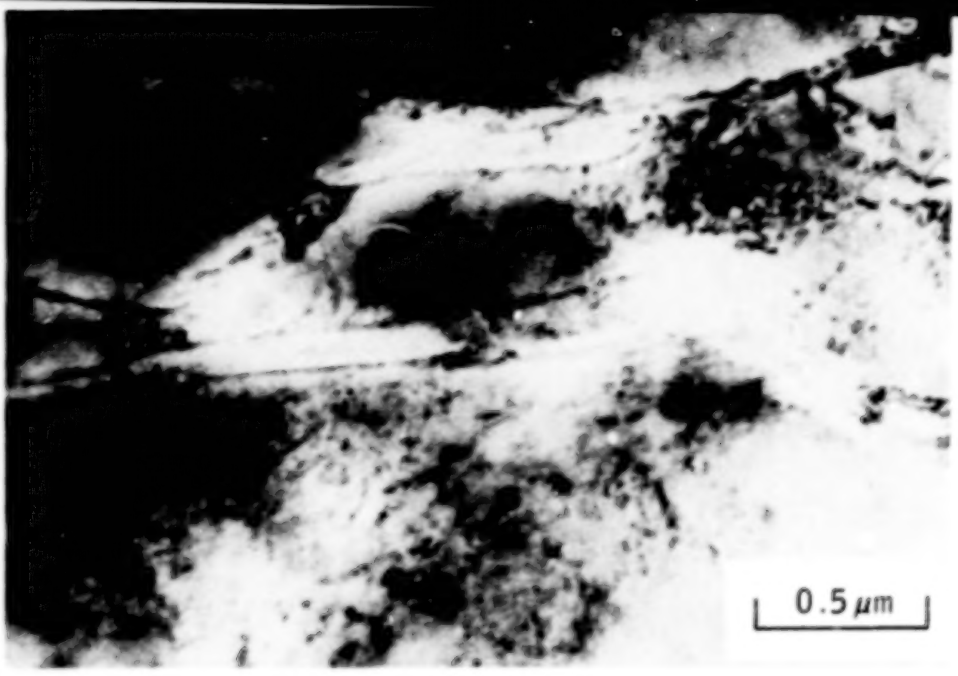

(a) Bright field image showing martensitic substructure. Precipitation of cementite not obvious.

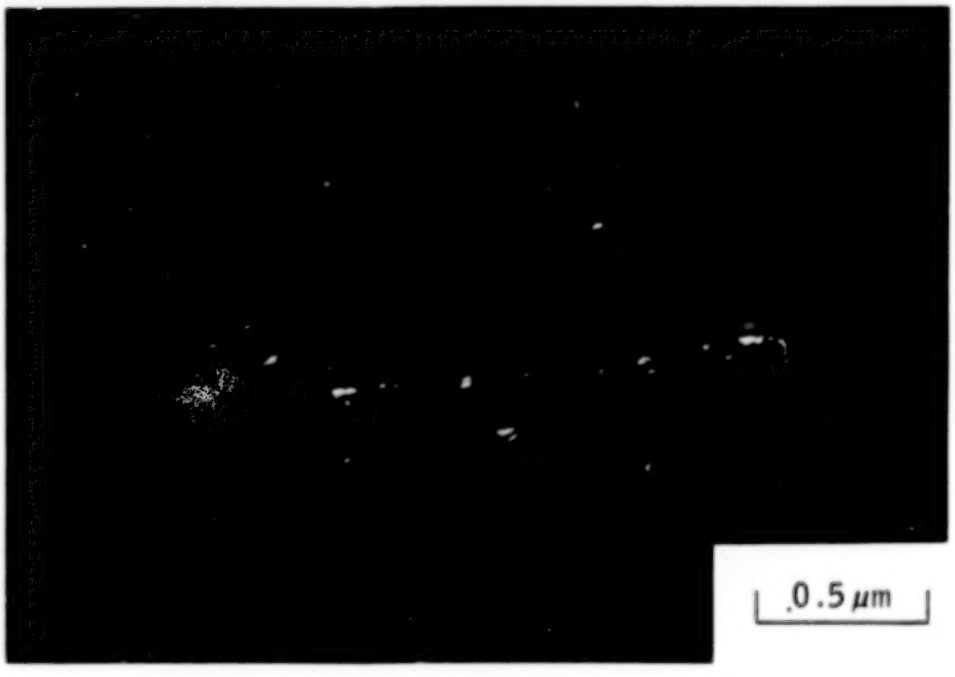

(b) Dark field image, in which imaging of a cementite reflection reveals cementite precipitates.

Figure 10.- Bright field and dark field images of 300M steel specimen austenitized and quenched from 1144 K (1600° F) and double tempered at 700 K (800° F).

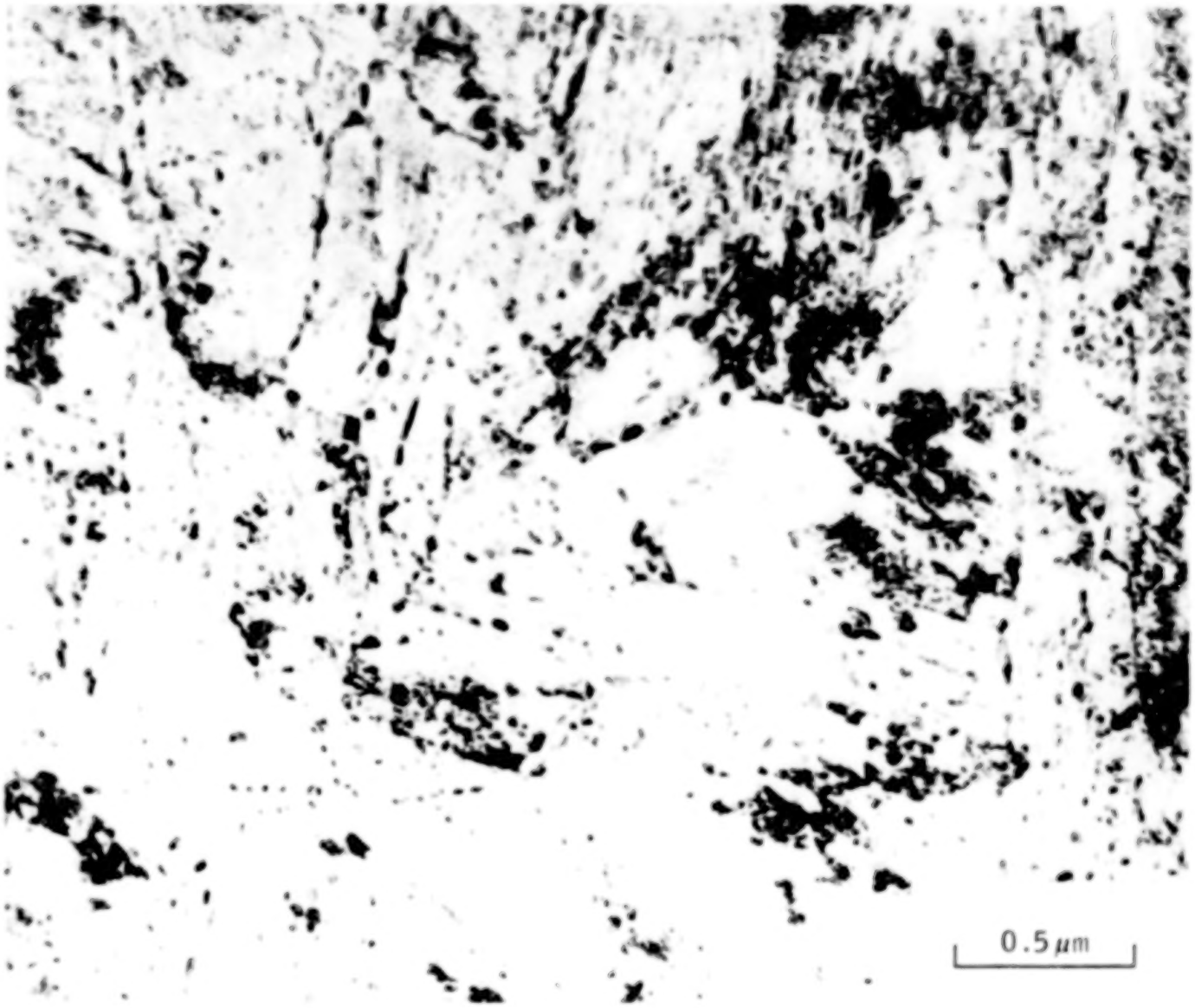

Figure 11.- Bright field image of 300M steel specimen austenitized at 1477 K (2200° F) and double tempered at 811 K (1000° F). Spheroidized cementite precipitates are shown at the lath and plate boundaries.

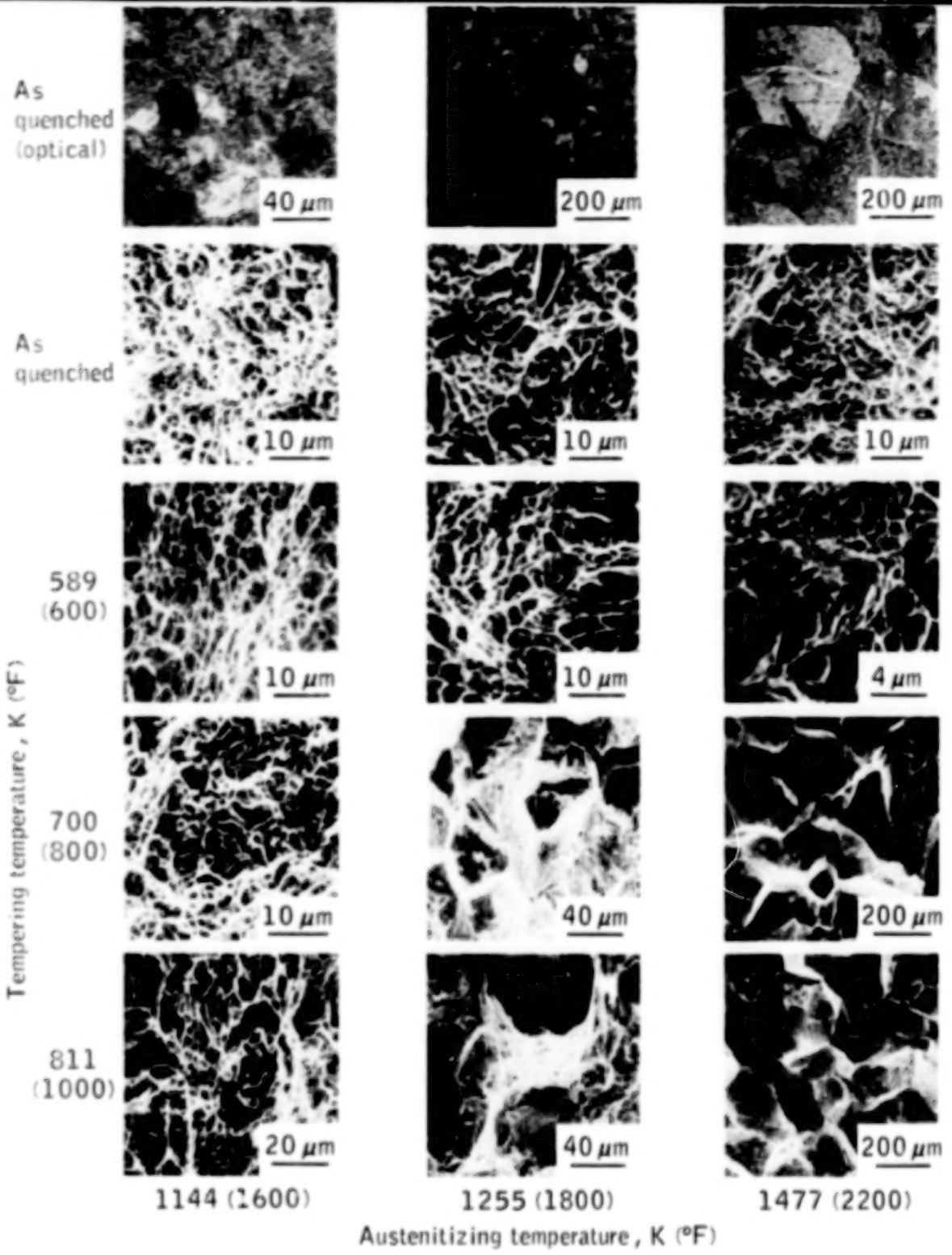

Figure 12.- Series of optical micrographs and scanning fractographs illustrating the fracture morphology of heat-treated and tested fracture toughness specimens. Optical micrographs are included for grain size reference.

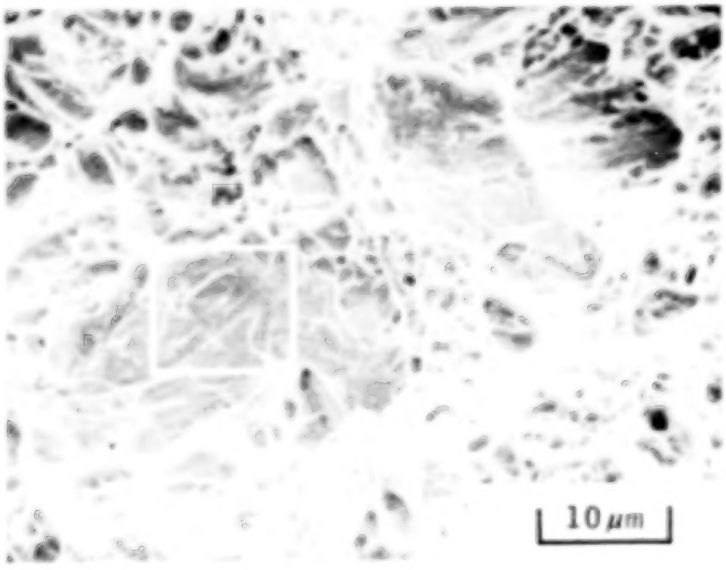

(a) Fractograph. Outlined area is shown in figure 13(b).

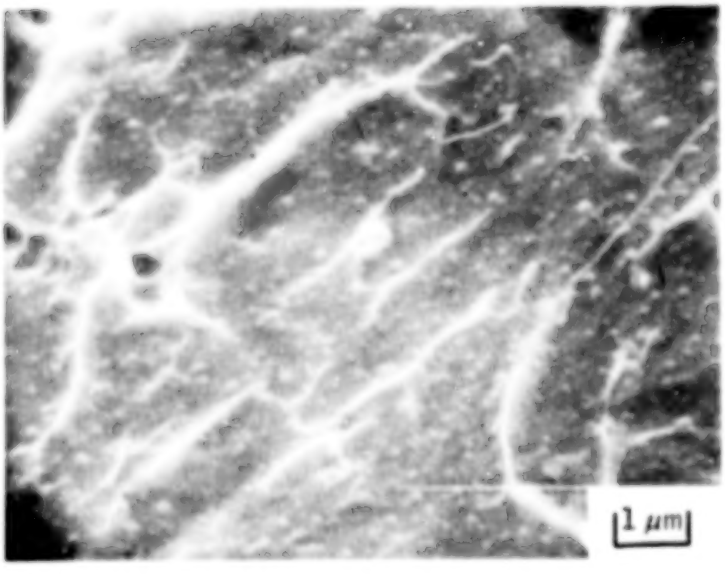

(b) Further enlargement of undissolved particles visible in figure 13(a).

Figure 13.- High-resolution fractograph showing concentration of undissolved particles on quasi-cleavage region of the fracture surface of a class A specimen austenitized at 1144 K (1600° F) and double tempered at 589 K (600° F).

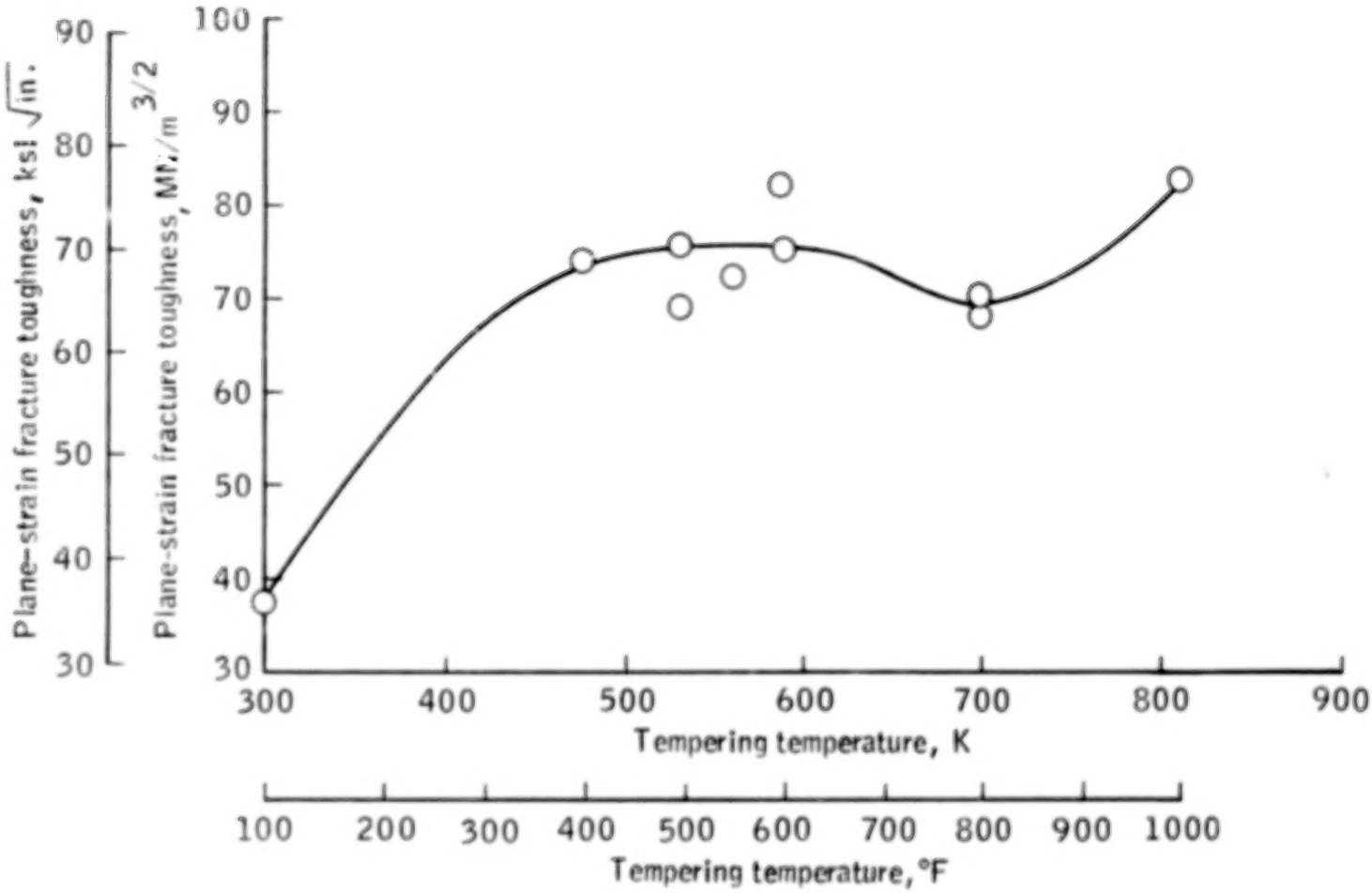

Figure 14.- Effect of tempering temperatures on plane-strain fracture toughness of 300M steel austenitized at 1200 K (1700° F).

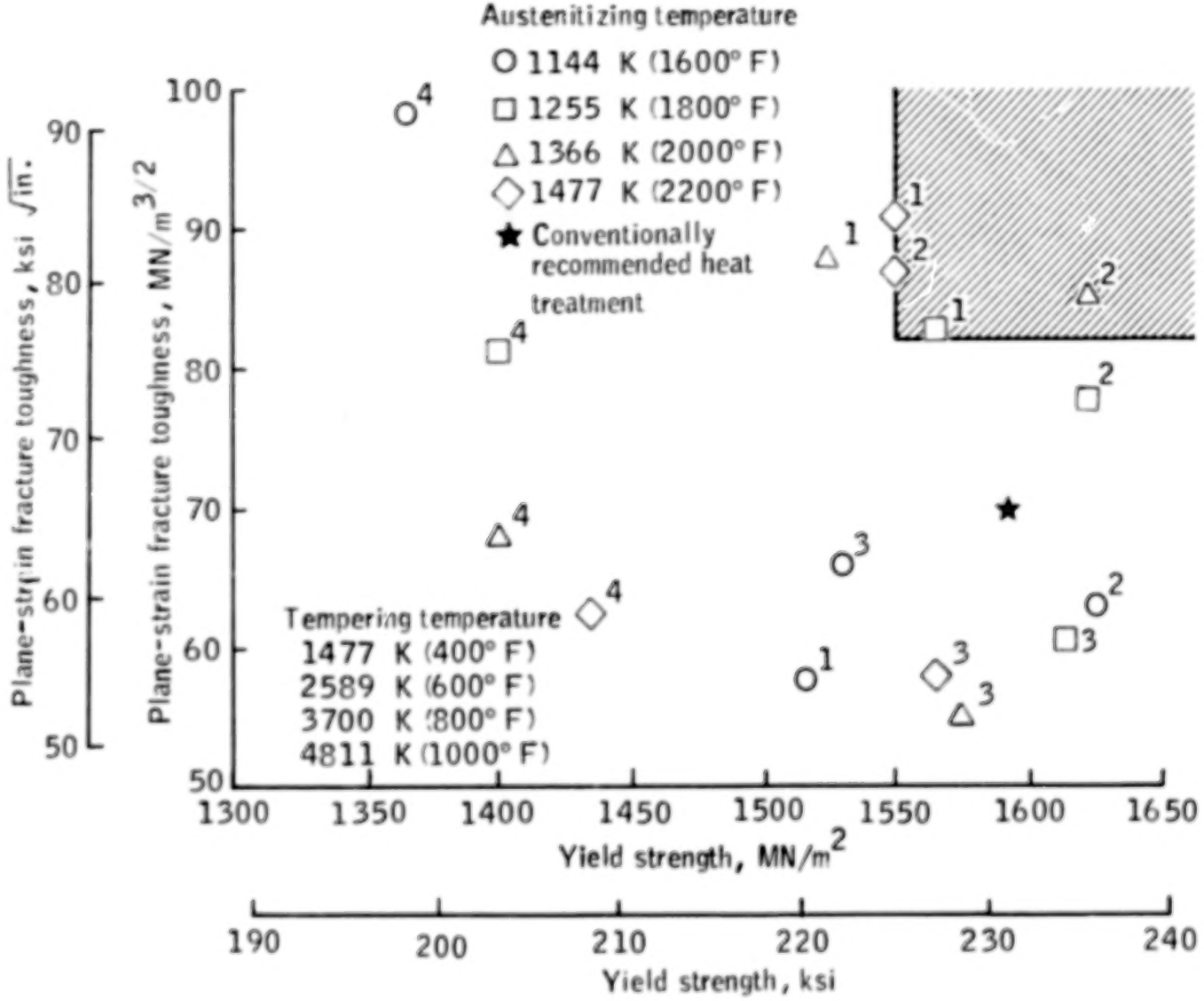

Figure 15.- Fracture toughness compared to yield strength for different heat treatments of 0.0127-meter (0.5 inch) thick 300M steel.

1. Report No.	2. Government Accession No.	3. Recipient's Catalog No.
NASA TP-1288		

4. Title and Subtitle	5. Report Date
MICROSTRUCTURE AND MECHANICAL PROPERTIES OF QUENCHED AND TEMPERED 300M STEEL	August 1978
	6. Performing Organization Code: JSC-13854
7. Author(s): J. I. Youngblood and M. Raghavan	8. Performing Organization Report No.: S-483
9. Performing Organization Name and Address: Lyndon B. Johnson Space Center, Houston, Texas 77058	10. Work Unit No.: 953-36-00-00-72
	11. Contract or Grant No.
12. Sponsoring Agency Name and Address: National Aeronautics and Space Administration, Washington, D. C. 20546	13. Type of Report and Period Covered: Technical Paper
	14. Sponsoring Agency Code

15. Supplementary Notes

16. Abstract

Type 300M steel, which is being used for the landing gear on the Space Shuttle Orbiter, was subjected to a variety of strength and toughness tests. Mechanical tests and microstructural studies were performed in parallel. The recommended austenitizing temperatures are given for both maximum plane-strain fracture toughness and maximum tensile ultimate and yield strengths.

17. Key Words (Suggested by Author(s))	18. Distribution Statement
High-strength steels Heat treat Fracture strength Yield strength Electron microscopes	STAR Subject Category: 39 (Structural Mechanics)

19. Security Classif. (of this report)	20. Security Classif. (of this page)	21. No. of Pages	22. Price*
Unclassified	Unclassified	40	$4.00

END

JAN 0 8 1979